EXAFS Studies of Some Alkoxydithiobenzoate Complexes of Zn(II) and Pd(II) in Their Liquid-Crystal Phases

Daniel Guillon,† Duncan W. Bruce,‡ Pascale Maldivi,§ Mohammed Ibn-Elhaj,† and Rupinder Dhillon‡

Groupe des Matériaux Organiques, Institut de Physique et Chimie des Matériaux de Strasbourg, ICS, 6 rue Boussingault, 67083 Strasbourg Cedex, France; Sheffield Centre for Molecular Materials, Department of Chemistry, The University, Sheffield S3 7HF, England; and CEA/Département de Recherche Fondamentale sur la Matière Condensée, CNRS/ Laboratoire de Chimie de Coordination (URA 1194), SESAM/CC, Centre d'Etudes Nucléaires de Grenoble, BP 85X, 38041 Grenoble Cedex, France

Received September 15, 1993. Revised Manuscript Received November 22, 1993®

One palladium and one zinc alkoxydithiobenzoate complex were studied both in the solid state and in their mesophases using the EXAFS technique. Analysis of the data provided information on the degree and nature of aggregation at the temperature of interest. In particular, the study has shown that zinc complexes which were dimeric in the solid state retained that dimeric nature in the mesophase. In the case of the palladium complexes, EXAFS showed that intradimer Pd–S interactions persisted through various crystal phases, before weakening in the crystal smectic phase and disappearing completely in the fluid SmC phase.

1. Introduction

Some of us have recently described the synthesis and mesomorphism of several metal complexes of 4-alkoxydithiobenzoates.[1] Single-crystal X-ray diffraction studies of two Zn(II) dithiobenzoate complexes ($[Zn_2(4\text{-odtb})_4]$ and $[Zn_2(8\text{-odtb})_4]$ (*n*-odtb represents an alkoxydithiobenzoate group where the alkyl chain has *n* carbon atoms) had shown that they existed as covalently-bonded dimers in the solid state (Figure 1) and that the coordination environment around the metal was similar to that found in related dialkyldithiocarbamate complexes of Zn(II), Cd(II), and Hg(II).[2] However, on dissolution in organic solvents such as toluene or chloroform, osmometric molecular weight measurements showed that these Zn(II) dithiobenzoates existed as monomers (again in common with the related dithiocarbamates). This observation posed a rather important question, namely, what was the species which gave rise to the observed mesomorphism in these materials (all of these complexes showed an enantiotropic nematic phase and, in addition, the homologues with n = 8, 9, and 10 showed a smectic C phase which was monotropic for n = 8)? Was the mesomorphic species a simple tetrahedral monomer, or did the mesomorphism arise from the dimeric species?

In addition to the Zn(II) complexes, some Pd(II) dithiobenzoates had also been synthesized. For the longer chain homologues, the phase behavior was characterized by the appearance of a crystal smectic phase followed by a SmC phase, before decomposition set in above 300 °C.

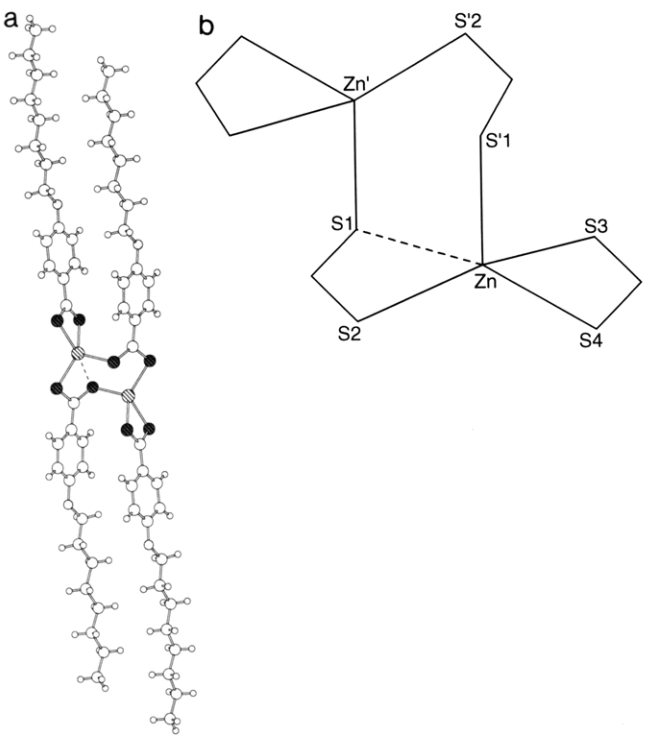

Figure 1. (a) Molecular structure of $[Zn_2(8\text{-odtb})_4]$. (b) Geometry of coordination and labeling of atoms around the central Zn atom of $[Zn_2(8\text{-odtb})_4]$.

Single-crystal X-ray analysis of one homologue, namely, $[Pd(8\text{-odtb})_2]$, showed that in the solid state the molecules were loosely associated as non-covalently-bound dimers through intermolecular Pd–S interactions at a distance of 3.38 Å (Figure 2). The literature on metal-containing liquid-crystal systems contains some debate on the presence and possible role of intermolecular metal/metal and/or metal/ligand interactions in determining the mesomorphism of coordinatively-unsaturated complexes. It was therefore of great interest to try to find out whether these interactions persisted through the various mesophases shown by the complex and therefore to try to

† Institut de Physique et Chimie des Matériaux de Strasbourg.
‡ The University.
§ Centre d'Etudes Nucléaires de Grenoble.
® Abstract published in *Advance ACS Abstracts,* January 1, 1994.

(1) Adams, H.; Albeniz, A. C.; Bailey, N. A.; Bruce, D. W.; Cherodian, A. S.; Dhillon, R.; Dunmur, D. A.; Espinet, P.; Feijoo, J. L.; Lalinde, E.; Maitlis, P.; Richardson, R. M.; Ungar, G. *J. Mater. Chem.* **1991**, *1*, 843.
(2) Bonamico, M.; Mazzone, G.; Vaciago, A.; Zambonelli, L. *Acta Crystallogr.* **1965**, *19*, 898. Iwasaki, H. *Acta Crystallogr., Sect. B.* **1973**, *29*, 2115. Iwasaki, H.; Ito, M.; Kobayashi, K. *Chem. Lett.* **1978**, 1399. Domenicano, A.; Torelli, L.; Vaciago, A.; Zambonelli, L. *J. Chem. Soc. A* **1968**, 1351.

0897-4756/94/2806-0182$04.50/0

understand what effect such interactions might have on mesomorphic properties.

To address these questions, extended X-ray absorption fine structure (EXAFS) was selected as a suitable technique. EXAFS methods[3] have been found to be very useful for the study of metal coordination environments, providing information on the nature and number of atoms around the metal of interest at distances of up to 4–5 Å. More recently, EXAFS has been applied to the study of metal-containing liquid-crystal systems. For example, the metal environment around Cu and Rh in the columnar systems $[M_2(RCO_2)_4]$ (M = Cu or Rh) has been studied[4,5] in addition to the Cu environment in some copper salicylaldimato complexes.[6]

For the present study, two complexes were chosen for which single crystal data already existed, namely $[Zn_2(8\text{-odtb})_4]$ and $[Pd(8\text{-odtb})_2]$. Their mesomorphic behavior is described below. However, in the case of the Pd complex, an additional crystal–crystal transition is reported at 96 °C. Many of these dithiobenzoate complexes have extensive crystal polymorphism, and this was not reported in the original paper as it did not contribute to the discussion of the properties of the materials:

$[Pd(8\text{-odtb})_2]$

$$K \xrightarrow{70\,^\circ C} K' \xrightarrow{96\,^\circ C} K'' \xrightarrow{107\,^\circ C} \text{cryst S} \xrightarrow{215\,^\circ C} SmC \xrightarrow{315\,^\circ C} I$$

$[Zn_2(8\text{-odtb})_4]$

$$K \xrightarrow{80\,^\circ C} K' \xrightarrow{147\,^\circ C} N \xrightarrow{184\,^\circ C} I$$

$$SmC \xleftarrow{140\,^\circ C} N$$

K, K′, and K″ are for crystalline phases, cryst S for an ordered crystalline smectic phase, SmC for the smectic C phase, N and I for the nematic and isotropic phases, respectively.

Data were recorded at several temperatures below the crystal smectic phase, in the crystal smectic phase and in the SmC phase. For the zinc complex, data were recorded at two temperatures below the nematic phase and in the nematic phase. In both cases, each temperature below the S phase (for Pd) or N phase (for Zn) corresponded to a slightly different crystalline modification as identified by microscopy and DSC methods.[1]

2. Experimental Section

2.1. Sample Preparation. Samples (about 50 mg) were pressed (under a pressure of about 5×10^6 g cm^{-2}) into pellets of dimensions 28 × 5 × 0.5 mm, which were carefully checked for homogeneous thickness and absence of cracks or holes. The pellets were then placed in tight boron nitride cells with thin (0.1 mm) windows. The cells were inserted within the heating unit designed for X-ray absorption measurements.[5] The temperature was regulated within 1 °C.

2.2. Data Collection. The EXAFS experiments were run on beamline "EXAFS 1" at LURE (Orsay). The experimental setup used has been described elsewhere.[7] The X-ray beam was obtained from the DCI storage ring under the usual running conditions: 1.85 GeV, a maximum stored current of 250 mA, and a (331)-Si-channel-cut monochromator. Data were collected in transmission mode; the direct beam and scattered beam intensities were measured with ionization chambers, filled with air for the experiments at the Zn K-edge and with argon for the studies at Pd K-edge. Energy resolution was estimated to be about 0.5 eV for the experiments performed at the zinc edge, and 4 eV for the experiments performed at the palladium edge. The energy calibrations were monitored using a zinc foil and a sample of one of our palladium complexes. The energy scanning was obtained through rotation of the monochromator. Some typical absorption spectra, obtained at the palladium and zinc edges, are shown in Figure 3.

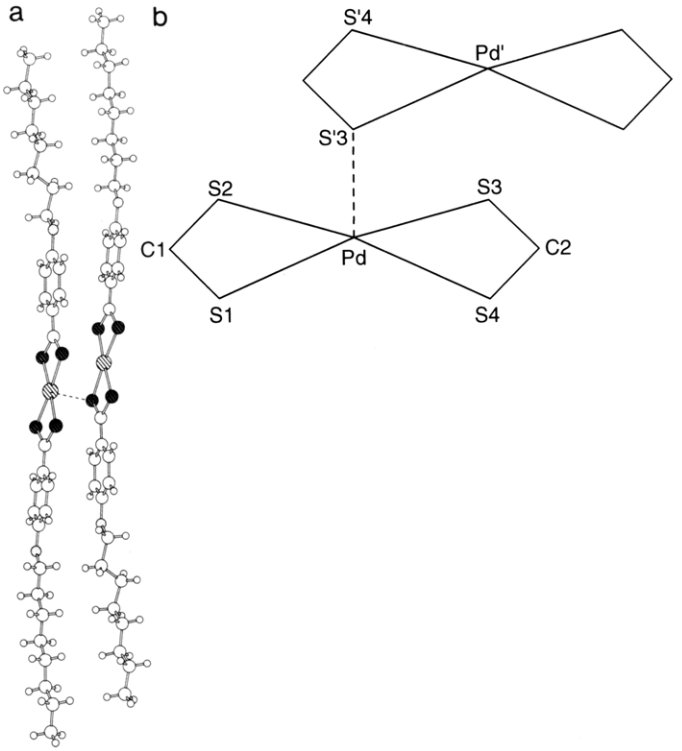

Figure 2. (a) Molecular structure of $[Pd(8\text{-odtb})_2]$. (b) Geometry of coordination and labeling of atoms around the central Pd atom of $[Pd(8\text{-odtb})_2]$.

2.3. Data Analysis. The EXAFS spectra were analyzed by classical procedures,[7] using programs provided by Bonnin et al.[8] In a first step, the absorption μ_1 before the edge was perfectly fitted with a linear function and the atomic absorption coefficient μ_0 was fitted with a spline function. The EXAFS signal corresponding to the atom shells around the metal atoms was then extracted from the experimental spectra using the following normalization relationship:

$$\chi(E) = ((\mu - \mu_1) - \mu_0)/\mu_0$$

The energy edge value has been defined as being the energy corresponding to the maximum of the $\mu(E)$ derivative. For the Fourier transform of the Zn EXAFS spectra, a Kaiser–Bessel window (with $\tau = 3$) between 3.8 and 14 Å^{-1} was used together with a k^3 weighting factor; for the Pd EXAFS spectra, the Fourier transform was obtained with a Kaiser–Bessel window ($\tau = 3$) between 3 and 13.5 Å^{-1} and a k^1 weighting factor. In each pseudoradial distribution, the main peaks were analyzed in order to obtain the filtered EXAFS spectra of the corresponding shells. It is important to note that the reality of the peaks has been checked through the variation of τ (when a peak is real, it should exist whatever the value of τ).

In a second step, the values of backscattering amplitudes and phases were deduced using the known crystallographic data determined at room temperature or taken from the tables of McKale.[9] In a third and final step, these amplitudes and phases were used to determine the local distribution of scatterers around

(3) Teo, B. K. In *EXAFS: Basic Principles and Data Analysis*; Springer-Verlag: Berlin, 1986.
(4) Ibn-Elhaj, M.; Guillon, D.; Skoulios, A.; Maldivi, P.; Giroud-Godquin, A. M.; Marchon, J. C. *J. Phys. Paris* **1992**, *2* (12), 2237.
(5) Maldivi, P.; Guillon, D.; Giroud-Godquin, A. M.; Marchon, J. C.; Abied, H.; Dexpert, H.; Skoulios, A. *J. Chim. Phys.* **1989**, *86*, 1651.
(6) Albertini, G.; Guido, A.; Mancini, G.; Stizza, S.; Ghedini, M.; Bartolino, R. *Europhys. Lett.* **1990**, *12*, 629.
(7) Raoux, D.; Petiau, J.; Bondot, P.; Calas, G.; Fontaine, A.; Lagarde, P.; Levitz, P.; Loupias, G.; Sadoc, B. *Rev. Phys. Appl.* **1980** *15*, 1079.
(8) Bonnin, D.; Kaiser, P.; Fretigny, C.; Desbarres, Ecole d'été du CNRS, Garchy, 1988.

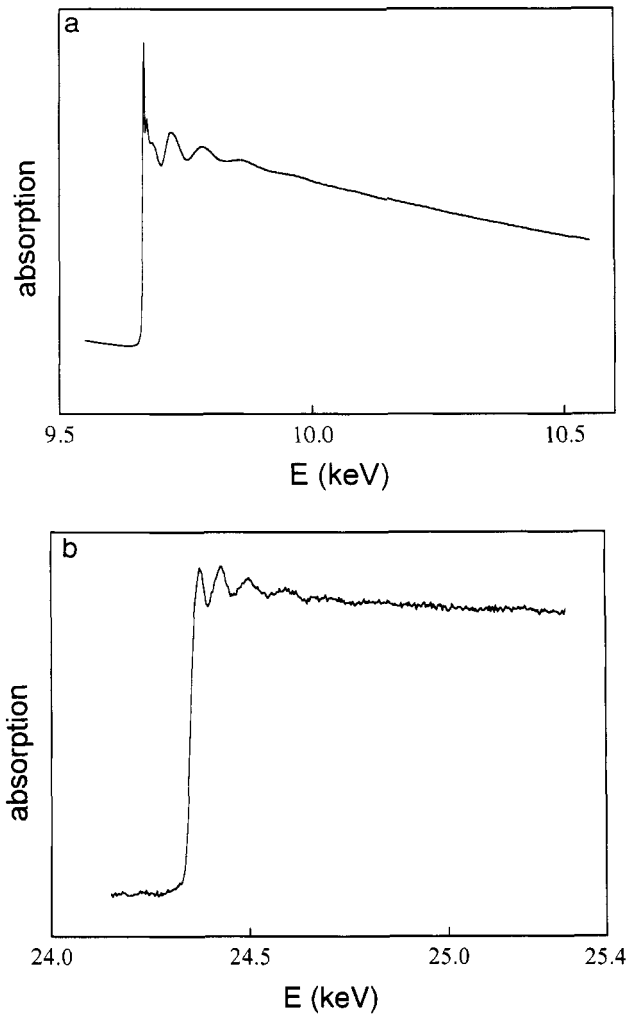

Figure 3. K-edge zinc and palladium EXAFS absorption spectra at room temperature of (a) $[Zn_2(8\text{-odtb})_4]$ and (b) $[Pd(8\text{-odtb})_2]$.

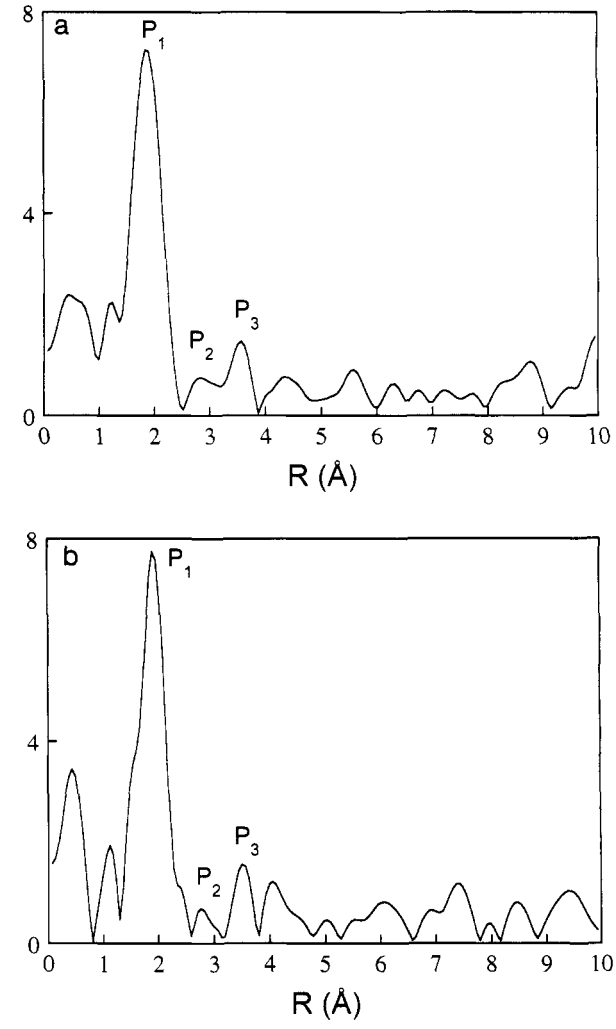

Figure 4. Pseudoradial distributions around the palladium atom in the crystalline phases: (a) K phase at 27 °C; (b) K′ phase at 100 °C.

the metal atoms, as well as their radial distance therefrom, in the different phases of these two compounds as a function of temperature. Relevant interatomic distances for the two reference compounds are shown in Table 1.

Let us recall that the accuracy relative to the distances is about 5–10% and that relative to the number of atoms is only around 20%. Finally, it is important to note that the number of independent points $N_{idp} = 2D(k)D(R)/p = 6$; for this reason, only two of the four theoretical parameters were allowed to vary during the fits, so that the number of fit parameters never exceeded the number of independent points.

3. Results and Discussion

3.1. $[Pd(8\text{-odtb})_2]$. In the crystalline phases of this compound, EXAFS spectra were recorded at 25, 72, and 100 °C. The corresponding pseudoradial distributions are shown in Figure 4. Three peaks (P_1, P_2, and P_3) are clearly present and centered at 1.90, 2.88, and 3.56 Å, respectively. It has to be noted that peaks P_2 and P_3 are not well separated and should be analyzed as a whole. The results obtained using both the crystallographic data of this compound (see the main interatomic distances around Pd atom in Table 1) and the theoretical values of the backscattering amplitudes and phases given by McKale[9] are essentially identical. Thus, it was possible to assign peak P_1 to the covalently-bound four equatorial sulfur atoms (S1, S2, S3, S4; see Figure 1), P_2 to the two carbon atoms (C1, C2) and to the loosely-associated sulfur atom (S′3), and P_3 to the palladium atom (Pd′) and one sulfur atom (S′4) of a neighboring molecule.

Table 1. Radial Distances of Atoms A from Metal Atoms As Determined Crystallographically for $[Zn_2(8\text{-odtb})_4]$ and $[Pd(8\text{-odtb})_2]$

$[Zn_2(8\text{-odtb})_4]$

atom A	Zn–A dist (Å)	shell	atom A	Zn–A dist (Å)	shell
S2	2.37	P1	S1	2.84	P2
S3	2.37	P1	Zn′	3.81	P3
S′1	2.37	P1	S′2	4.21	P3
S4	2.50	P1			

$[Pd(8\text{-odtb})_2]$

atom A	Pd–A dist (Å)	shell	atom A	Pd–A dist (Å)	shell
S1	2.32	P1	C2	2.84	P2
S2	2.32	P1	S′3	3.38	P2
S3	2.32	P1	Pd′	3.94	P3
S4	2.32	P1	S′4	4.13	P3
C1	2.84	P2			

The peaks so identified were properly filtered and back-Fourier-transformed into "experimental" EXAFS spectra corresponding to two or three atomic shells, depending whether P_2 and P_3 were analyzed separately or not. These experimental spectra were then refined using the general EXAFS theory[10] (Figure 5). The adjustable parameters used in the theoretical calculations are the number (N) of given atoms, their radial distance (R) to the palladium

(9) McKale, A. G.; Knapp, G. S.; Chan, S. D. *Phys. Rev.* **1986**, *B33*, 841. McKale, A. G.; Veal, B. W.; Paulikas, A. P.; Chan, S. D.; Knapp, G. S. *J. Am. Chem. Soc.* **1988**, *110*, 3763.

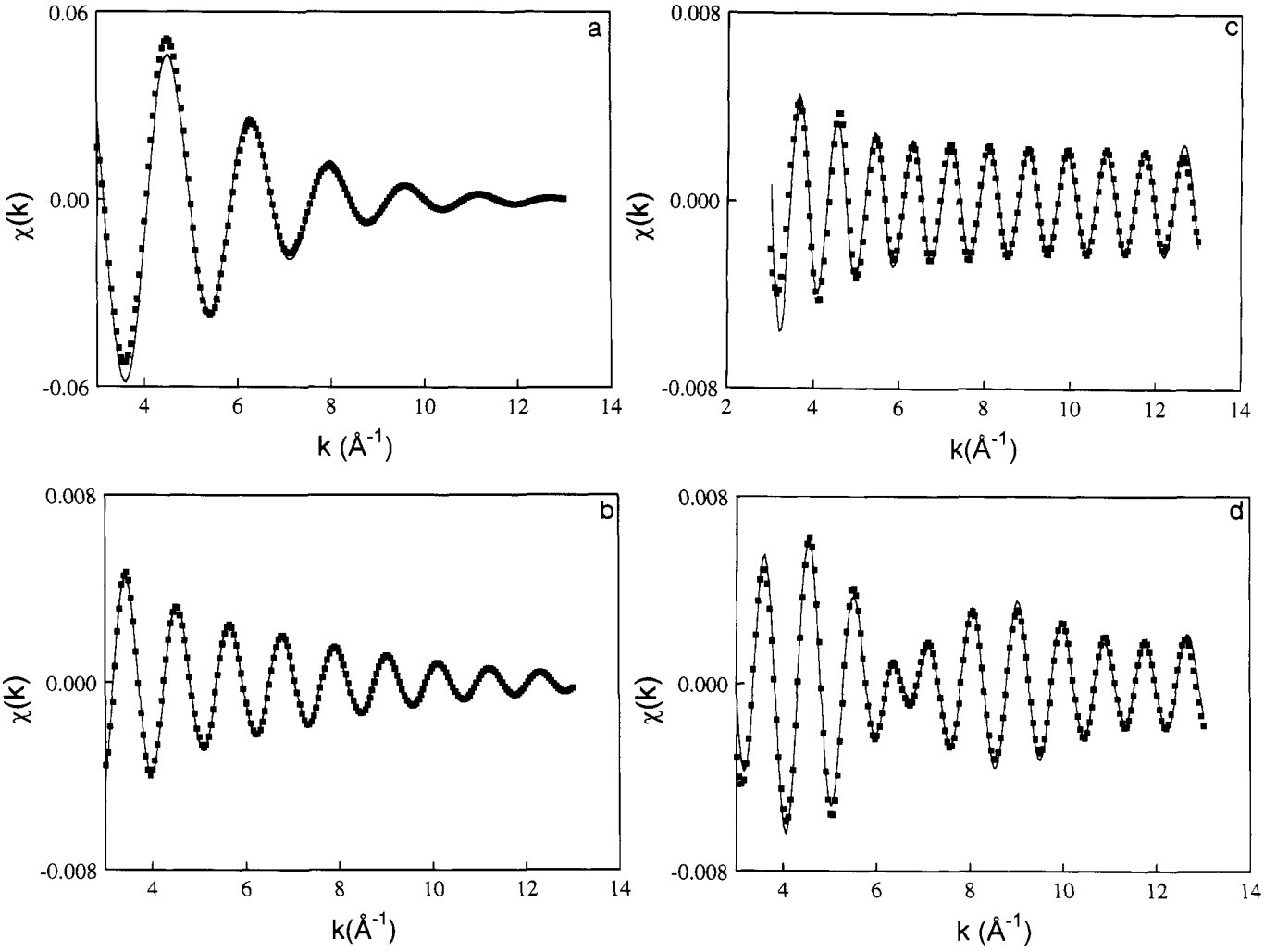

Figure 5. Comparison of experimental (points) and calculated (lines) EXAFS spectra for [Pd(8-odtb)$_2$] at 27 °C: (a) shell P_1, (b) shell P_2, (c) shell P_3, (d) shells P_2 and P_3.

Table 2. EXAFS Parameters of [Pd(8-odtb)$_2$] in the Crystalline K (27 °C) and K′ (72 and 100 °C) Phases (Parameters Defined in the Text)

T (°C)	atoms	N	R (Å)	$\Delta\sigma$ (Å)	ΔE_0 (eV)	$\Delta\chi(k) \times 10^5$
27	S	4.0	2.34	0.08	−5.02	8.5
	C	2.0	2.93	0.06	−18.7	9.9
	S	1.0	3.20	0.05	−9.62	
	Pd′	1.0	3.83	0.002	8.28	15.0
	S	1.1	4.28	0.07	7.34	
72	S	4.0	2.34	0.08	5.15	7.8
	C	2.0	2.78	0.21	−16.23	41.0
	S	1.0	3.11	0.05	−8.9	
	Pd′	1.0	3.72	0.06	14.25	20.0
	S	1.0	4.17	0.09	14.23	
100	S	4.0	2.34	0.02	−3.70	8.0
	C	2.0	2.71	0.10	−0.80	
	S	1.0	3.2	0.07	−1.16	90.0
	Pd′	1.0	3.75	0.05	14.20	25.0
	S	1.0	4.17	0.11	14.20	

atom, the deviation ($\Delta\sigma$) of the Debye–Waller effect, the energy shift (ΔE_0) of the K-edge; the corresponding reliability factor is $\Delta_\chi(k) = \sum(\chi_{exp} - \chi_{th})^2/\sum(\chi_{exp})^2$. The final adjusted values are reported in Table 2.

Let us point out that the interatomic distances thus found are in good agreement with those found in the previous crystallographic data[1] (see Table 1); note also that the EXAFS spectrum $\chi(k)$ shows a maximum located around 9 Å^{-1} (see Figure 5d); this maximum in the decreasing regime of $\chi(k)$ as a function of k is a typical signature of metal–metal interactions, and as a result of Pd–Pd interactions in our particular case. The spectra registered at 72 and 100 °C in the K′ phase lead to the same overall structure with interatomic distances smaller than those determined at 27 °C (see Table 2).

For the crystal smectic phase, the pseudoradial distribution recorded at 150 °C (Figure 6a) shows three peaks P_1, P'_2, and P'_3 which are now well resolved and centered at 1.90, 2.76, and 3.38 Å, respectively. P_1 always corresponds to the four bound sulfur atoms (S1, S2, S3, S4), but the main difference lies in the fact that P'_2 can be fitted only as a shell containing only two carbon atoms at 3.04 Å, and P'_3 to a shell containing only one sulfur atom at 3.77 Å. The most striking evidence of a different intermolecular organization in the smectic phase comes from the filtered spectrum of the two peaks P'_2 and P'_3, where no maximum of $\chi(k)$ around 9 Å^{-1} could be observed (Figure 7b): this is the signature of the absence, within these two shells, of any palladium atom located at a distance similar to that of the crystalline phase.

The pseudoradial distribution of the crystal smectic phase (Figure 6a) shows also another peak (P_4) centered at 4.6 Å. The analysis of the peak P_4 which was filtered between 3.93 and 4.97 Å shows clearly the existence of a palladium atom at 4.7 Å and another sulfur atom at 4.9 Å (the peak P_4 was not analyzed in the previous crystalline

(10) Ashley, C. A.; Doniach, S. *Phys. Rev.* **1975**, *B11*, 1279. Lytle, F. W.; Sayers, D.; Stern, E. *Phys. Rev.* **1975**, *B11*, 4836. Lee, P. A.; Pendry, J. B. *Phys. Rev.* **1975**, *B11*, 2795.

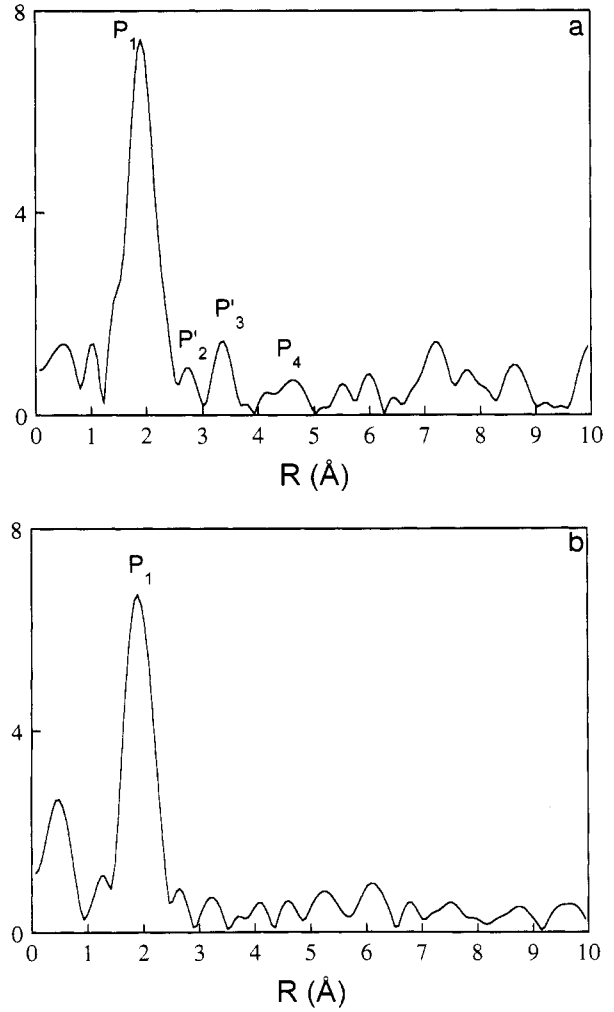

Figure 6. Pseudoradial distributions around the palladium atom: (a) in the crystal smectic phase at 150 °C, (b) in the smectic C phase at 240 °C.

Table 3. EXAFS Parameters of [Pd(8-odtb)$_2$] in the Crystal Smectic (150 °C) and in the Smectic C (240 °C) Phases (Parameters Defined in the Text)

T (°C)	atoms	N	R (Å)	$\Delta\sigma$ (Å)	ΔE_0 (eV)	$\Delta\chi(k) \times 10^5$
150	S	4.0	2.35	0.09	−10.60	16.0
	C	2.0	3.04	0.01	0.96	76
	S	1.0	3.77	0.01	2.50	
	Pd′	1.0	4.69	0.01	1.10	30.0
	S	1.0	4.91	0.11	−5.70	
240	S	4.0	2.37	0.08	−9.84	28

spectra, since it corresponded only to low atomic weight atoms).

For the smectic C phase, the pseudoradial distribution (see Figure 6b) obtained from the spectra registered at 240 °C, shows mainly one peak, P_1; it shows also other peaks of very low intensity for which attempts to find a palladium atom were unsuccessful. Indeed, it was possible to obtain a good fit between the experimental spectrum and the calculated one only for P_1 which contains the same sulfur atoms S1, S2, S3, and S4. Once more, this clearly shows that there are no longer any intermolecular interactions between palladium and sulfur atoms and therefore no more dimeric species in the fluid Sm C phase.

From the study above, it is clear that the mesomorphism of this palladium complex goes in parallel with the disappearance of intermolecular interactions. In the crystal smectic phase, the intermolecular interactions become weaker when compared to the crystalline state,

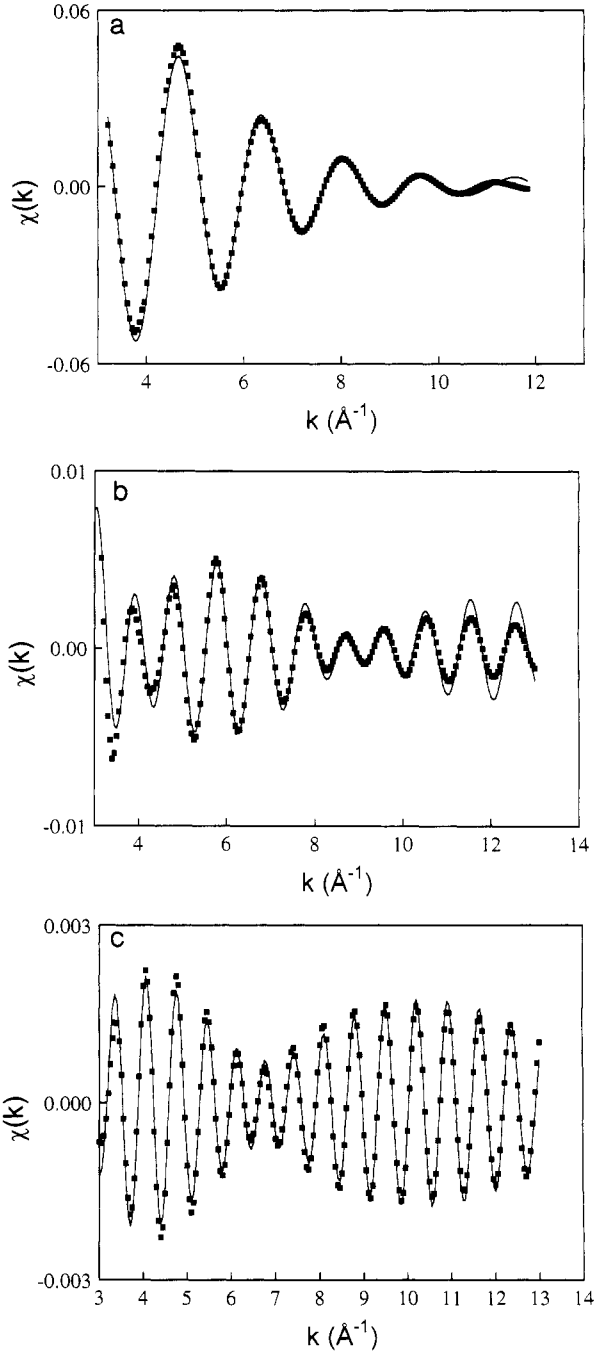

Figure 7. Comparison of experimental (points) and calculated (lines) EXAFS spectra for [Pd(8-odtb)$_2$]: at 150 °C in the crystal smectic phase (a) shell P_1, (b) shell P'_2 and P'_3, (c) shell P_4.

and the intermolecular palladium–sulfur distance was, on average, 3.77 Å, compared to 3.38 Å in the dimer in the crystalline phase. In the smectic C phase, these interactions lose completely their strength and then the molecules act individually.

3.2. [Zn$_2$(8-obtb)$_4$]. In the solid state of this compound, EXAFS spectra were recorded at 24 and 100 °C, corresponding to two different polymorphic crystalline phases. The corresponding pseudoradial distributions are shown in Figure 8. At 25 °C, two peaks (P_1 and P_2) are clearly present and centered at 2.03 and 2.64 Å, respectively; at 100 °C, three peaks (P_1, P_2, and P_3) can be identified and centered at 2.03, 2.64, and 3.93 Å, respectively. At 24 °C, P_1 was assigned to correspond to four sulfur atoms (three at 2.35 and one at 2.50 Å), and P_2 to one sulfur at 2.87 Å. At 100 °C, P_1 corresponds also to four sulfur atoms, P_2 to

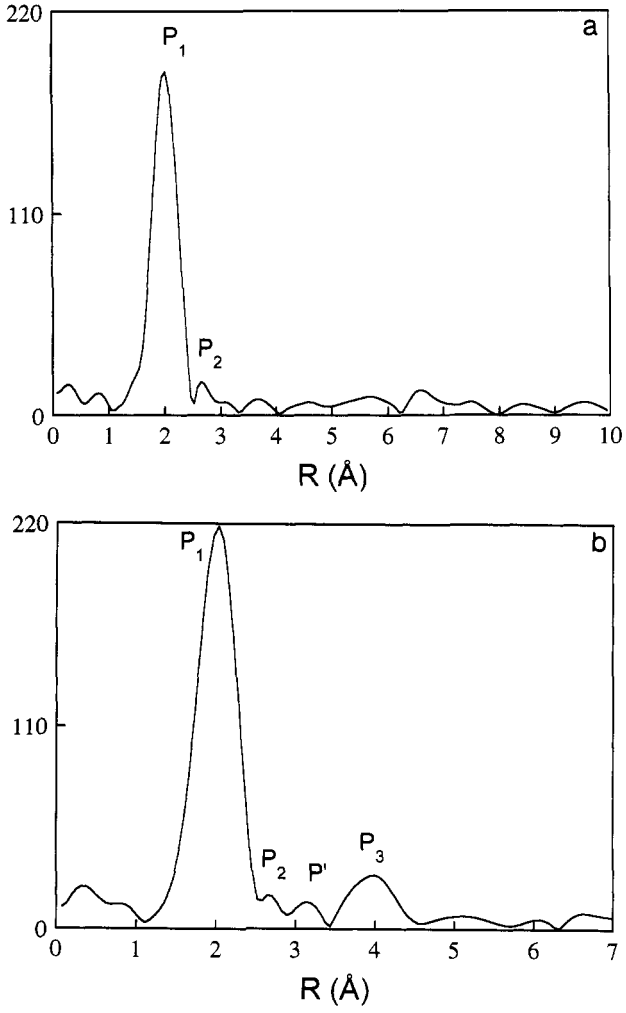

Figure 8. Pseudoradial distributions around the zinc atom in the crystalline phases of $[Zn_2(8\text{-odtb})_4]$: (a) K phase at 25 °C and (b) K′ phase at 100 °C.

Table 4. EXAFS Parameters of Recrystallized $[Zn_2(8\text{-odtb})_4]$ at 25, 100, and 160 °C (Parameters Defined in the Text)

T (°C)	atoms	N	R (Å)	$\Delta\sigma$ (Å)	ΔE_0 (eV)	$\Delta\chi(k) \times 10^6$
25	S	3.0	2.35	0.08	−7.00	0.6
	S	1.0	2.50	0.08	−3.70	
	S	1.0	2.87	0.07	−5.70	1.6
100	S	3.0	2.35	0.09	−7.80	0.1
	S	1.0	2.50	0.11	−8.90	
	S	1.0	2.90	0.12	−5.50	
	Zn′	1.0	4.05	0.09	−15.00	12
	S	1.0	4.19	0.10	−15.00	
160	S	3.0	2.35	0.09	−10.80	0.4
	S	1.0	2.54	0.08	−11.70	
	S	1.0	2.85	0.20	−11.10	
	Zn′	1.0	3.88	0.09	−6.15	12
	S	1.0	4.19	0.09	−4.41	

one sulfur atom, and P_3 to one Zn and one sulfur atoms; in the particular case of that temperature, one can observe another peak P′, centered at 3.3 Å, between P_1 and P_3 (see Figure 8b); however, it has not been considered further in the analysis, since it corresponds only to carbon atoms.

The peaks so identified were properly filtered and back-Fourier-transformed into experimental EXAFS spectra, which were then refined by using either the phases and amplitudes extracted from the crystallographic data or the phases and amplitudes given by McKale. The final adjusted values are reported in Table 4. Let us point out that at 100 °C, P_1 and P_2 were fitted together (see Figure 9a), since they were located close to each other in the

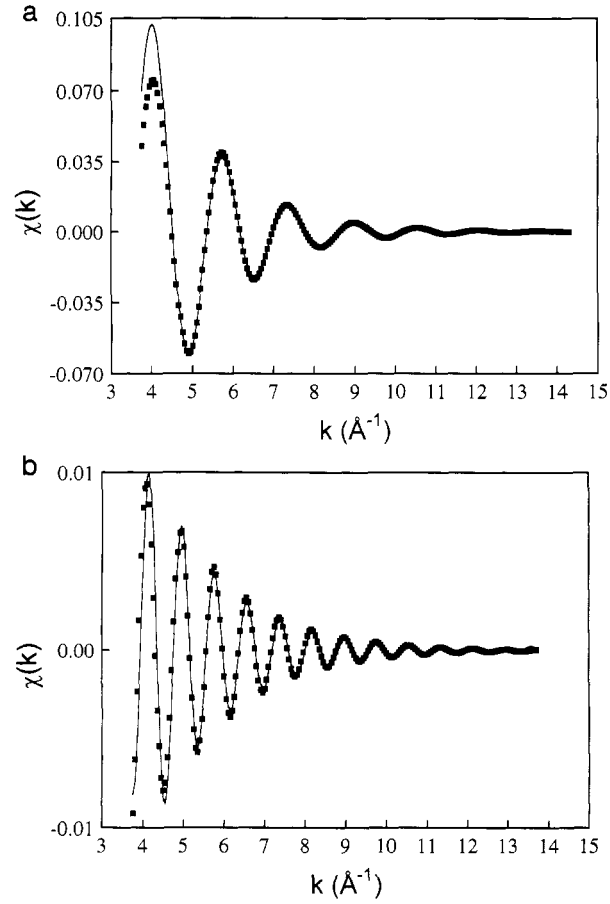

Figure 9. Comparison of experimental (points) and calculated (lines) EXAFS spectra for $[Zn_2(8\text{-odtb})_4]$: at 100 °C in the crystalline K′ phase (a) shell P_1 and P_2 (b) shell P_3.

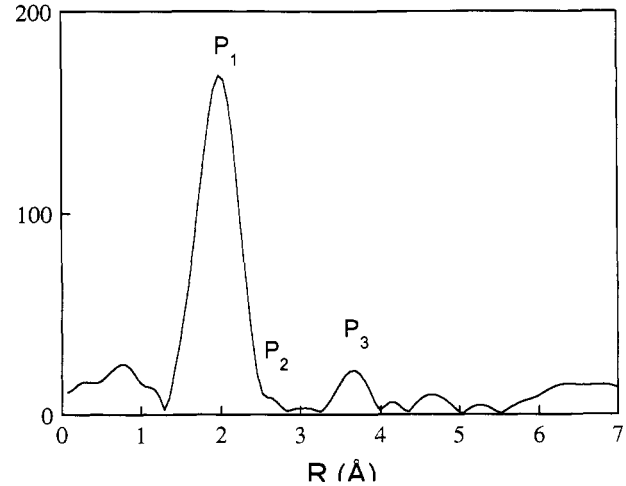

Figure 10. Pseudoradial distributions around the zinc atom in the nematic phase of $[Zn_2(8\text{-odtb})_4]$ at 160 °C.

pseudoradial distribution. It is interesting to note that the parameters, and especially the number of neighbors around the Zn atom and the corresponding interatomic distances, are in good agreement with the crystallographic data recorded at room temperature, indicating that the dimeric species are still present in the high-temperature crystalline phase.

The EXAFS spectra registered at 160 °C in the nematic phase lead to a pseudoradial distribution which is very similar to that obtained at 100 °C in the crystalline phase, with a P_2 peak closer to P_1 (see Figure 10). The values found for the adjustable parameters found (see Table 4) show that the geometry of coordination around the Zn

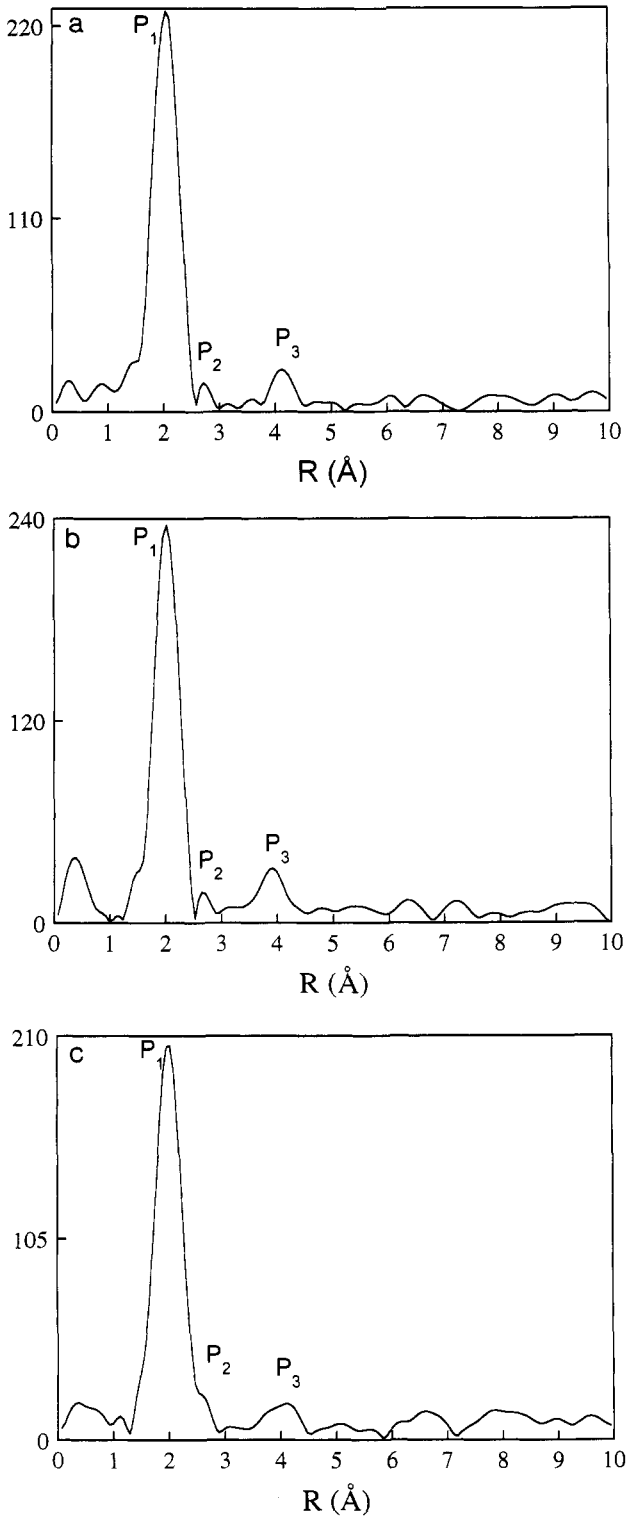

Figure 11. Pseudoradial distributions around the zinc atom in the crystalline phases of $[Zn_2(8\text{-odtb})_4]$ powder: (a) at 34 °C, (b) at 80 °C, and (c) at 120 °C.

atom in the crystalline phase is preserved in the nematic phase, indicating that the Zn complexes do exist as dimers even in the nematic phase at high temperature.

3.3. $[Zn_2(8\text{-odtb})_4]$ Powder. In a previous study of the Zn complexes, it has been observed that the mesomorphism of the orange powders obtained directly from the synthesis was different from that found after recrystallization of the sample, although elemental analysis showed both to have the same composition. Thus, while the red crystals of the Zn complexes gave a well-defined mesomorphism, the orange powders behaved in a different

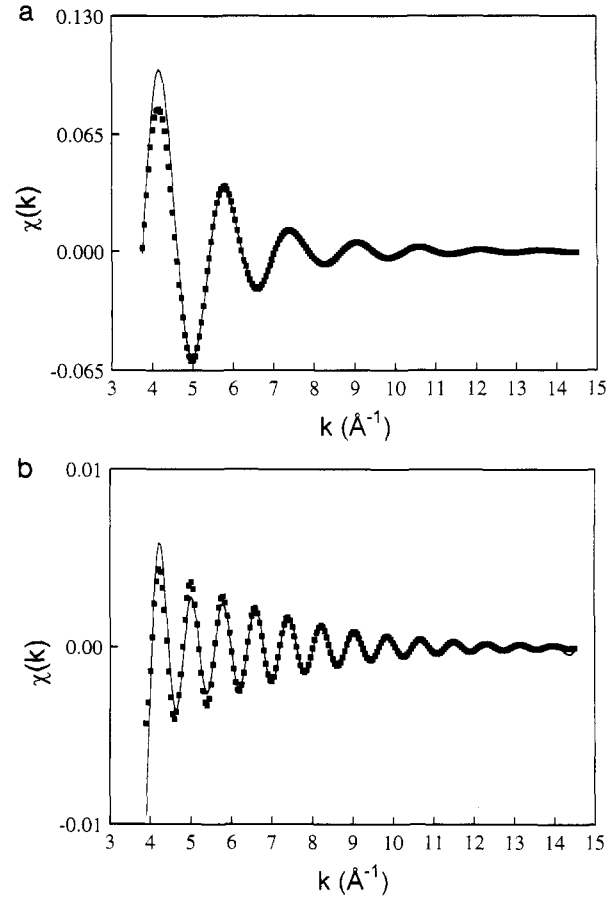

Figure 12. Comparison of experimental (points) and calculated (lines) EXAFS spectra for $[Zn_2(8\text{-odtb})_4]$ powder at 80 °C in the crystalline phase (a) shell P_1 and P_2 (b) shell P_3.

manner and appeared to consist of two materials with immiscible mesophases. It has been suggested that this may be due to the presence of both a dimeric and a monomeric form. We therefore subjected a sample of the orange powdered form of $[Zn_2(8\text{-odtb})_4]$ to analysis by EXAFS at three temperatures (34, 80, and 120 °C) in the solid state; no spectrum at higher temperature has been registered in the mesomorphic state, owing to a leak problem in the cell.

The spectra have been analyzed in the same manner as for the recrystallized $[Zn_2(8\text{-odtb})_4]$ sample (see section 3.2). The corresponding pseudoradial distributions are shown in Figure 11 and the comparison between the experimental data (at 80 °C) and the theoretical spectra in Figure 12; the adjusted EXAFS parameters are given in Table 5. It is interesting to note that at 34 °C, the distance between Zn atoms is 4.12 Å, whereas it was only 3.85 Å in the recrystallized sample at a similar temperature in the K phase. Even if the variation in the distance can be attributed to the accuracy of its determination (5–10%), these results seem however to suggest that the crystalline phase obtained at room temperature for the $[Zn_2(8\text{-odtb})_4]$ powder may correspond to the K′ phase obtained from the recrystallized sample, although further experiments would be required to confirm this point. This does not, however, help to understand the difference in mesomorphism between the two forms.

4. Conclusion

The present study has further demonstrated the utility of EXAFS for the examination of metal-containing liquid

Table 5. EXAFS Parameters of $[Zn_2(8\text{-odtb})_4]$ Powder at 34, 80, and 120 °C (Parameters Defined in the Text)

T (°C)	atoms	N	R (Å)	$\Delta\sigma$ (Å)	ΔE_0 (eV)	$\Delta\chi(k) \times 10^5$
34	S	3.0	2.37	0.08	−11.73	0.5
	S	1.0	2.54	0.08	−5.30	
	S	1.0	2.91	0.09	−0.84	
	Zn′	1.0	4.12	0.22	−0.02	8.6
	S	1.0	4.25	0.05	−18.16	
80	S	3.0	2.37	0.08	−12.87	0.9
	S	1.0	2.54	0.06	−6.25	
	S	1.0	2.95	0.09	−1.35	
	Zn′	1.0	4.03	0.07	−20.88	6.8
	S	1.0	4.26	0.10	−17.75	
120	S	3.0	2.36	0.08	−11.96	0.3
	S	1.0	2.55	0.05	−11.77	
	S	1.0	2.76	0.26	11.37	
	Zn′	1.0	4.11	0.08	−19.80	31.0
	S	1.0	4.22	0.06	−21.40	

crystals in their mesophases. In particular, the study has shown that zinc complexes which were dimeric in the solid state retained that dimeric nature in the mesophase. Such an observation is interesting as the shape of mesogenic species is somewhat different from most of the metal-containing liquid crystals known[11] in having a relatively open central core, formed by the M–S–C–S–M–S–C–S ring. The relative disposition of the rings and chains, however, is akin to that found in the orthopalladated azobenzenes described by Ghedini.[12]

In the case of the palladium complexes, EXAFS showed that intradimer Pd–S interactions persisted through various crystal phases, before weakening in the crystal smectic phase and disappearing completely in the fluid SmC phase. Thus in this case, it is demonstrable that intermolecular metal–metal or metal–ligand interactions play no part in stabilization of the liquid crystal phase of the complex.

Acknowledgment. We would like to thank the Royal Society (D.W.B.), the SERC (R.D.), the British Council for financial support, Mme Françoise Villain for experimental assistance, and Johnson Matthey for generous loans of palladium.

(11) Bruce, D. W. In *Inorganic Materials*; Bruce, D. W., O'Hare, D. Wiley: Chichester, 1992.
(12) Ghedini, M.; Pucci, D.; Cesarotti, E.; Antogniazza, P.; Francescangeli, O.; Bartolino, R. *Chem. Mater.* **1993**, *5*, 883.